

## ARTICLE

# Amino Acid Intercalated Montmorillonite: Electrochemical Biosensing Applications

Cite this: DOI: 10.1039/x0xx00000x

Filiz Demir<sup>a</sup>, Bilal Demir<sup>a</sup>, Esra E. Yalcinkaya<sup>b</sup>, Serdar Cevik<sup>c</sup>, Dilek Demirkol<sup>a</sup>, Ulku Anik<sup>c</sup>, Suna Timur<sup>a,\*</sup>Received 00th January 2012,  
Accepted 00th January 2012

DOI: 10.1039/x0xx00000x

www.rsc.org/

The present work is the first work that includes the use of glycine (Gly), lysine (Lys) and glutamic acid (Glu) modified clay mineral matrices in the biosensors. For this purpose, initially, Gly, Lys and Glu were intercalated with montmorillonite (Mt), thus, various modified Mts were obtained. These modified materials were then characterized via X-ray diffraction, Fourier transform infrared spectroscopy, zeta potential and thermal gravimetric analysis (TGA/DTG) and scanning electron microscopy (SEM). In order to investigate the applicability of amino acid modified clay minerals in biosensor area, glucose oxidase (GOx) was selected as the model enzyme and GOx based biosensor was prepared. After immobilizing the enzyme with amino acid modified Mt onto a glassy carbon electrode, working conditions like pH and modifier type were optimized. Among the modified Mts, Gly-Mt was the optimum clay mineral type and pH 4.0 was the optimum pH value. Then analytical characteristics were examined under optimum experimental conditions. Linear range of optimum sensor design was 0.1 – 1.0 mM within kinetic parameters of immobilized enzyme  $K_m^{app} = 0.7$  mM,  $I_{max} = 107.8$  nA. Finally, developed biosensor was applied to real samples where the results were compared with a spectrophotometric reference method.

## 1 Introduction

In the last decade, there is a growing interest towards combining inorganic clay nanocomposites within enzyme or cells by taking the advantage of physical and chemical properties. These materials can be used in many biological applications including biosensors, drug release and cell adhesion.<sup>1–7</sup> The crystal structure, morphology and chemical composition of clays offer ion exchange capacity, good thermal, mechanical and chemical stabilities and advanced adsorption properties. Because of this, they can be used as a suitable immobilization platform for the facile biosensing transducer.<sup>8</sup>

Phyllosilicates are 2:1 layered structure consisting of an octahedral sheet which is predominantly occupied by trivalent or divalent cations (i.e.  $Al^{3+}$  or  $Mg^{2+}$ ) sandwiched between two tetrahedral siliceous sheets. Vermiculites and smectites that include montmorillonite (Mt), nontronite and laponite are typical clay minerals and belonging to phyllosilicate family. As cationic clay mineral, Mt exhibits some unique characteristics like intercalation, swelling and strong adsorption.<sup>9</sup> In addition to that, Mt can be an appropriate natural silicate which can be utilized for encapsulant material in intercalation processes.<sup>10–11</sup> In this way, alkylammonium salts,<sup>3–12</sup> polymers<sup>13</sup> and amino acids (mostly hydrophobic amino acids)<sup>14</sup> have been used as the intercalating agents. On the other hand, these modifiers have enabled thermostability and improved mechanical strength to

clay minerals. Therefore, organo-modification of clay minerals has been drawing interest for clay modified electrode preparation and enzyme immobilization. However, clay mineral modified enzyme electrodes can suffer from enzyme leaching during the application. Hence, by adding the glutaraldehyde (GA) and bovine serum albumin (BSA) to the biofilm, a robust biosensing platform can be obtained.<sup>15–16</sup>

In many studies based on the intercalation of amino acids onto clay minerals, adsorption capacities of amino acids and their detailed characterization related to pH, temperature, interlayer spaces have been conducted with Fourier transform infrared spectroscopy, X-ray diffraction, thermogravimetric analysis and zeta potential.<sup>17–22</sup> However, it can be seen that not so much work reported in the literature for the application of amino acid modified clay minerals, particularly in biosensor areas. Avinash et al. (2011) reported the unnatural amino acid (5-aminovaleric acid) modified Mt and their use in tissue engineering via forms biocomposites with hydroxyapatite.<sup>23</sup> Also in another study, Wang et al. (2013) synthesized and characterized the  $Ga^{3+}$ -salicylidene-amino acid (glycine, alanine, tyrosine, phenylalanine, aspartic acid and glutamic acid, respectively) schiff base complexes with layered double hydroxides to evaluate potential applications of drug delivery system for antimicrobial activity.<sup>24</sup>

Present study consists of the intercalation of Mt with glycine, lysine and glutamic acid amino acids, their detailed characterization and application to biosensors. In biosensing

experiments, amino acid modified Mts have been used as immobilization materials for glucose oxidase (GOx) adsorption onto Mt layers via GA+BSA support as proposed in previous work based on histidine modified Mt based Laccase biosensor.<sup>25</sup> After the electrochemical characterization, optimization and determining the analytical parameters, the most efficient sensor design was applied to real samples.

## 2 Material and Method

### 2.1 Reagents and Apparatus

Glucose oxidase (GOx; EC 1.1.3.4, 50 U/mg protein), D-(+) - glucose, bovine serum albumin (BSA), glycerol, glutaraldehyde (GA) solution (25%, v/v) were purchased from Sigma Chem. Co. (St. Louis, MO, USA; www.sigmaaldrich.com). The clay mineral used for the experiments was obtained from West Anatolia. It was purified from bentonite before use. Particles, 2  $\mu\text{m}$  in diameter were obtained by sedimentation (ion-exchange capacity; 92 meq 100  $\text{g}^{-1}$ ). Amino acids (Glycine, glutamic acid and lysine) were purchased from Sigma Chem. Co. (St. Louis, MO, USA). All other chemicals were used of reagent grade.

PalmSens Potentiostat (Palm Instruments, Houten, Netherlands) and FRA 2  $\mu$ -AUTOLAB Type III (ECO CHEMIE Instruments B.V., Netherlands) were used for amperometric, impedimetric and voltammetric measurements. A three electrode cell where clay mineral modified electrodes as working electrode, Ag/AgCl electrode with 3.0 M KCl as a reference electrode and platinum (PT) as the counter electrode was used. Pharmacia LKB Novaspec II spectrophotometer was used for the spectrophotometric measurements.

For the characterization, all samples were first examined with X-ray diffraction (XRD) Spectrometers (Philips E'xpert Pro; Cu-K $\alpha$  radiation,  $\lambda=1.541 \text{ \AA}$ ) to determine the interlayer spaces of Mt and Mod-Mts. The XRD spectra were obtained at a scanning rate of 2.00  $\text{min}^{-1}$  and the  $2\theta$  angles ranged from 5.00–80.00. The basal spacing values of pure Mt and Mod-Mts were calculated by Bragg's law. Fourier transform infrared (FTIR) spectra of clay minerals were recorded using a Perkin Elmer Pyris 1 FTIR Spectrometer on KBr plates. Thermal degradation was studied with a thermogravimetric analyzer (Perkin Elmer Pyris 1 TGA/DTA) by heating the samples from ambient temperature to 1000  $^{\circ}\text{C}$  at 10  $^{\circ}\text{C min}^{-1}$  under a 10 bar dry air atmosphere. The electrokinetic properties of clay minerals were determined by measuring the zeta-potential of particles with a Zeta-Meter 3.0+ (with a Zeiss DR microscope, GT-2 type quartz cell, molybdenum-cylinder anode, and platinum-rod cathode electrode). The clay mineral samples were stirred overnight in the deionized water to obtain well dispersed particles. The zeta potential of the modified Mt dispersions was estimated from the measured electrophoretic mobilities by employing the Smoluchowski equation.<sup>26</sup> The zeta potential assigned to the dispersions was the average of the data obtained from at least 10 experiments. The surface morphology was monitored with a FEI Quanta250 FEG scanning electron microscope (SEM). An accelerating voltage

of 5.0 kV was applied for each sample, and a spot size of 3 was used. All of the samples were dried in a vacuum oven before the analyses at 50  $^{\circ}\text{C}$  for 2 days.

### 2.2 Modification of organo-montmorillonite

In order to have a successful development of clay mineral-based biosensors, it is necessary to chemically modify a naturally hydrophilic silicate surface to an organophilic one so that it can be compatible with a chosen enzyme. The modified Mt was prepared by the method of ion exchange. Sodium-Mt powder (0.5 g) was dispersed in 200 mL deionized water under stirring with a Heidolph magnetic stirrer for about 24 h. The glutamic acid (Glu), lysine (Lys) and glycine (Gly) amino acids were separately dissolved in 20 mL deionized water. The amounts of amino acids were equivalent to 2 times the CEC of Mt. These intercalating agents were firstly protonated with 1.0 M HCl aqueous solutions to adjust the pH to 2.0–3.0. Then, it was slowly dropped into the Mt dispersion for stirring 24 h at room temperature. The modified Mts (Glu-Mt, Lys-Mt and Gly-Mt) were separated by filtration and washed several times with deionized water until no chloride ions were detected by AgNO<sub>3</sub> solution. The obtained organic Mt was dried in a vacuum oven at 50  $^{\circ}\text{C}$  for 2 days. After the 2 days, the weight loss has not been observed.

### 2.3 Fabrication of A.A-Mt/GOx biosensors

Initially, GCE was polished with alumina slurry (0.05  $\mu\text{m}$  sized) and then bath sonication was applied for 5 min in ethanol:distilled water (1:1) solution. To construct the enzyme electrode, 5.0  $\mu\text{L}$  of Mt solution (1.0  $\text{mg mL}^{-1}$ ), 0.5 mg GOx (which is equal to 25 U), 2.5  $\mu\text{L}$  of BSA (1.0  $\text{mg mL}^{-1}$ ) and 2.5  $\mu\text{L}$  of GA (5.0%) were mixed. Afterwards, the mixture was spread over the electrode and allowed to dry at room temperature for 1 h.

All reagents were prepared in phosphate buffer (50 mM, pH 7.0). Prior to measurements, each daily prepared enzyme electrode was washed with distilled water to eliminate unbound enzyme.

### 2.4 Electrochemical Measurements

All amperometric experiments were performed in working buffer solution (10 mL). Electrodes were rinsed with distilled water and kept in sodium acetate buffer (50 mM, pH 4.0) for GOx biosensor at least 3 min after each trial. Enzyme immobilized electrodes were initially equilibrated in the buffer and then, the substrate (glucose) was added to the reaction cell. During the measurement of GOx electrode, an enzymatic reaction proceeds on two half reactions namely a reduction and a following oxidative step. In the first step, GOx which is a dimeric protein containing one tightly bound flavin adenine dinucleotide (FAD) per monomer as cofactor, catalyzes the oxidation of  $\beta$ -D-glucose to D-glucono-d-lactone, which is spontaneously converted to gluconic acid and in the second

step, the reduced GOx(FADH<sub>2</sub>) is reoxidized by oxygen to yield H<sub>2</sub>O<sub>2</sub>. In GOx, FAD acts as an electron acceptor, and it is reduced to FADH<sub>2</sub>; the FADH<sub>2</sub> is then oxidised by the final electron acceptor, molecular oxygen, with the oxygen being reduced to hydrogen peroxide (H<sub>2</sub>O<sub>2</sub>).<sup>27</sup> The decrease in the amount of oxygen in bioactive layer is monitored at -0.7 V with respect to Ag/AgCl electrode as a result of enzymatic activity. The biosensor responses were registered as the current signal (nano or  $\mu$ -A). The buffer was refreshed after each measurement. All chronoamperometric measurements were performed 3 times. Data were presented as the mean  $\pm$  standard deviation (S.D).

Cyclic voltammetry (CV) experiments and electrochemical impedance spectroscopy (EIS) measurements were performed on a FRA 2  $\mu$ -AUTOLAB Type III electrochemical measurement system from ECO CHEMIE Instruments B.V., (Netherlands) driven by NOVA software (www.ecochemie.nl). EIS measurements were performed in sodium phosphate buffer (50 mM, pH 6.5) containing 5.0 mM [Fe(CN)<sub>6</sub>]<sup>3-/4-</sup> with a frequency range from 0.1 Hz to 100 kHz at 0.2 V. CV measurements were conducted in the potential range of -0.4 V to 0.8 V with a 0.0244 V step potential and using only clay mineral film (without biological compound or cross-linker) in the presence of 0.1 M KCl used as the supporting electrolyte.

## 2.5 Sample Application

The biosensors were used to analyse the glucose content of some beverages. As a reference method, Trinder reagent which is a commercial enzyme assay kit was utilized for the analysis of the same samples spectrophotometrically. The method is based on the oxidation of glucose to D-gluconate by GOx with the formation of hydrogen peroxide. In the presence of peroxidase, a mixture of phenol and 4-aminoantipyrine is oxidized by hydrogen peroxide to form a red quinine imine dye proportional to the glucose concentration in the sample.<sup>28</sup>

## 3 Results and Discussion

### 3.1 Characterization of Organo-Modified Clay Minerals

The intercalation of organic-modified clay minerals was characterized by FTIR, XRD, and zeta potential measurements. Also, the thermal stability of pure and modified clay minerals was determined with TGA and DTG analysis. The nature of the chemical groups intercalated was investigated by FTIR and their spectra are shown in Fig 1. In the FTIR spectrum of Mt (Fig 1a), the band at 3630 cm<sup>-1</sup> is ascribed the -OH bond corresponding to the characteristic stretching for Al-Al-OH bond in the octahedral layer of Mt. The band at around 1630 cm<sup>-1</sup> is related with H-OH stretching vibration. An intense peak at 1054 cm<sup>-1</sup> is the characteristic absorption band for Mts corresponding to Si-O stretching. In the FTIR spectra of Mts (Fig 1b,c,d), characteristic absorption bands for both Mt and modifiers were observed. In addition to Mt band, the carbonyl group

(C=O) band of the amino acids that proves the modification were observed at 1700 cm<sup>-1</sup> at all FTIR spectra and in another work that was studied with natural amino acid intercalation of cloisite, the peaks for -COOH group in modified clay minerals support this FTIR results.<sup>29</sup> In addition to these bands, the bands around 1400 cm<sup>-1</sup> are attributed to the presence of N-H on the structure.

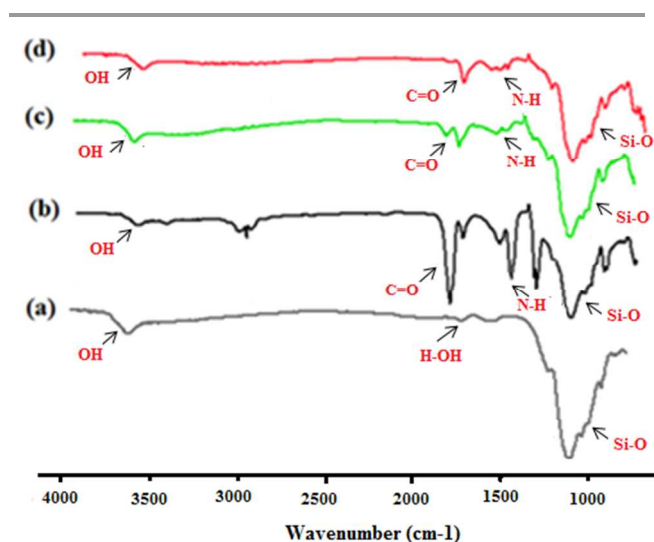


**Figure 1.** FTIR spectra of (a) Mt, (b) Glu-Mt, (c) Lys-Mt and (d) Gly-Mt.

The interlayer space and the crystalline configuration of the clay minerals can be identified by XRD. The basal spacing values of modified Mts were compared to pristine Mt to indicate the presence of amino acid molecules. Fig 2 shows the XRD patterns of Mt and amino acid modified Mts (Glu-Mt, Lys-Mt and Gly-Mt). According to the XRD pattern of Mt, the typical XRD reflection of Na<sup>+</sup>-Mt related to the basal spacing between the clay mineral layers appeared at 2 $\theta$ =7.74°. The basal spacing value of Mt was calculated as  $d_{001} = 11.4 \text{ \AA}$  from this value. For modified Mts, the peak at 7.74° shifts to 6.82°, 6.76° and 6.02° in the spectrum of Gly-Mt, Lys-Mt and Glu-Mt, respectively. This reflection appeared at the lower angles of the diffractogram indicated the intercalation of amino acid molecules in the interlayer spaces of Mod-Mts. The basal spacing of the modified Mts was calculated as  $d_{001} = 12.96, 13.06$  and  $14.67 \text{ \AA}$  for Gly-Mt, Lys-Mt and Glu-Mt, respectively. The swelling of modified Mts are 1.56, 1.66 and 3.27  $\text{\AA}$  for Gly-Mt, Lys-Mt and Glu-Mt, respectively. The increasing of basal spacing values of Mt could be seen clearly due to the increasing of the interlayer distance of the Mt with amino acids. It is attributed that the cation exchange process between the interlayer cations of Mt and amino acid salts was effectively carried out and amino acids intercalated into the Mt layers.

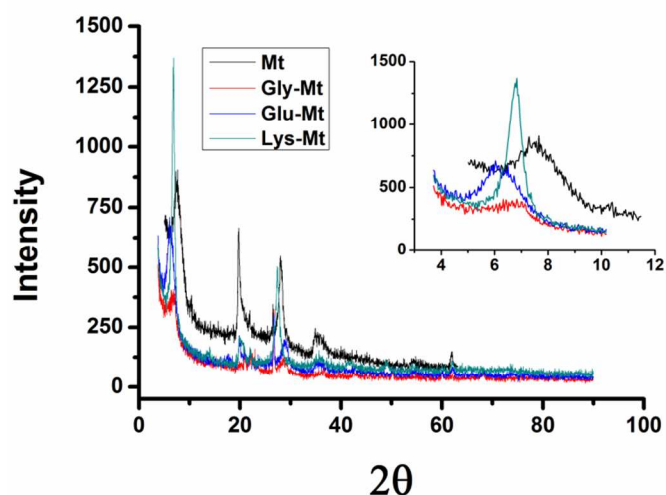


Figure 2. XRD patterns of Mt and Modified-Mts.

The thermal stability of Mt and amino acid modified Mts (Glu-Mt, Lys-Mt and Gly-Mt) was compared with TGA analysis. The TGA thermograms are shown in Fig. 3 a. Mt exhibited about 8.4% weight loss at 1000 °C because of the presence of volatile materials. Degradation started at 100 °C due to the unbounded H<sub>2</sub>O and continued up to about 800 °C due to the chemically bound H<sub>2</sub>O. The weight loss of the amino acid modified Mts was founded at 15.4, 17.4 and 21.5 weight % for Glu-Mt, Lys-Mt and Gly-Mt, respectively. The increasing of the weight loss was due to the adsorption of modifiers both at the surface and within the clay mineral layers. These results indicated that 6.0, 9.0 and 13.1 weight % (0.4, 0.6 and 1.7 mmole/g) of Glu, Lys and Gly as modifier were holding onto the Mt structure. For Gly-Mt, the percentage of ion exchange was calculated as 6.9% by using CEC of Mt that was lower from the TG data. This was indicated that Gly was adsorbed mostly on the clay mineral surface and also intercalated to the layers of Mt easily due to its un-branched and compact structure. However, the percentages of ion exchange were calculated as 13.5 and 13.4% for Glu-Mt and Lys-Mt, respectively by using CEC. It is evident that Glu and Lys amino acids could not intercalated to the layers of Mt easily according to the Gly amino acid due to its branched structure. Also, the thermal stability of the modified Mts was found lower than that of pristine clay mineral as our previous studies.<sup>4–12</sup>

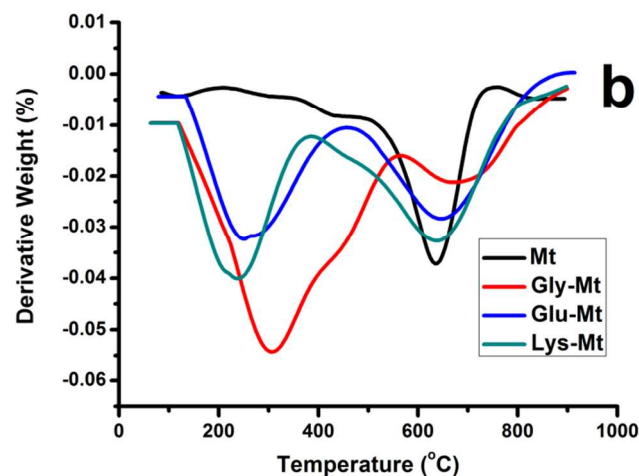
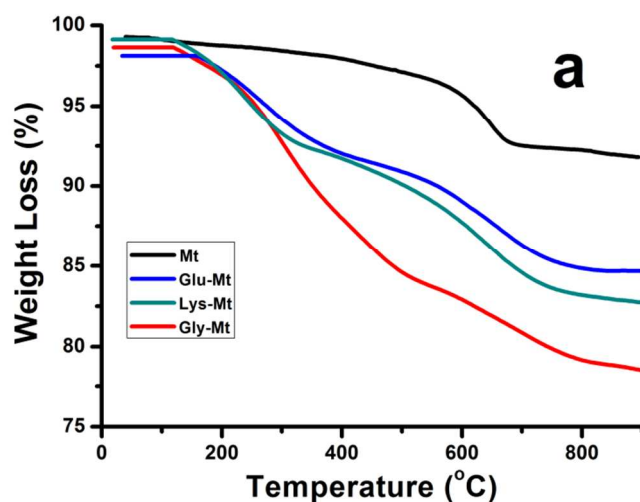


Figure 3. a) TG thermograms of Mt and Modified-Mts. b) DTG thermograms of Mt and Modified-Mts.

The DTG thermograms of the samples have already reported that the derivative of weight loss as a function of temperature in Fig 3 b. The max decomposition peak temperature of pure Mt was 635 °C from the thermogram of Mt. According to DTG thermograms of Glu-Mt, Lys-Mt and Gly-Mt, the two decomposition stages of modified Mts were between 100-800 °C. The first peak corresponding to the degradation of the intercalated species as Glu, Lys and Gly salts into Mt interlayer spaces. The max degradation peak temperatures of were 310, 250 and 235 °C for Glu-Mt, Lys-Mt and Gly-Mt, respectively. Hence, the Glu-Mt has the max degradation peak temperatures due to its structure. The second decomposition stages were occurred at about 640 °C due to the decomposition of clay mineral particles like with the pristine Mt.

When a solid surface is in contact with an aqueous solution, the formation of an interfacial charge causes a re-arrangement of the local free ions in the solution. The arrangement of the charges at the solid-liquid interface and the balancing counterions in the liquid is usually referred as the electrical



double layer. The zeta potential is an indicator of the surface charge properties of a colloid or a particle in solution and varies depending on the surface potential and the thickness of the electric double layer. It is usually characterized by the measurement of the electrophoretic mobility of the colloidal particles in dispersion which is a key technique for the determination of the surface properties of the particles.<sup>30</sup> The zeta potential can be used for studying and predicting colloidal stability and particle surface charge, effectively. It is also an important parameter for a number of applications including characterization of biomedical polymers, electrokinetic transport of particles or blood cells, sensors and biosensors, membrane efficiency and microfluidics.<sup>31–33</sup> In this study, the zeta potential of the Mts was calculated as  $-42.0 \pm 2.24$ ,  $-34.3 \pm 0.85$ ,  $-33.3 \pm 0.65$  and  $-30.3 \pm 0.43$  mV for Mt, Glu-Mt, Lys-Mt and Gly-Mt, respectively. After each modification step, the zeta potentials shifted to less-negative values as a result of adsorption of positively charged amino acid salts at the surface or interlayer of the mineral. Gly-Mt exhibited the lowest negative zeta potential value compared to that of the other amino acid modified clay mineral that it is compatible with TGA results.

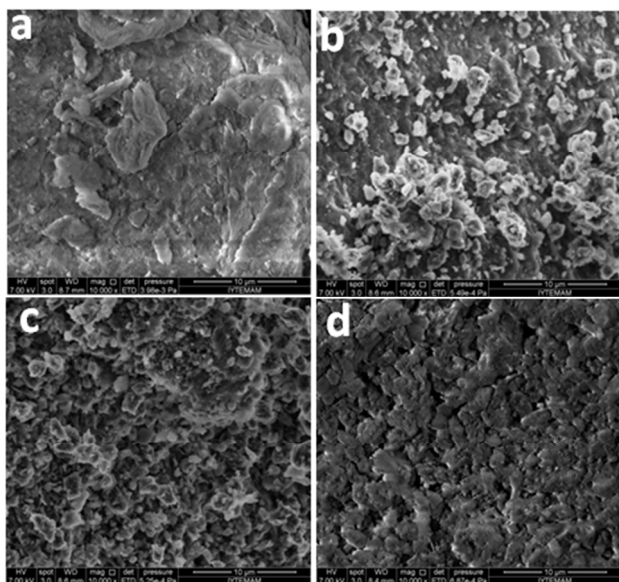


**Figure 4.** SEM images of (a) Mt, (b) Glu-Mt, (c) Lys-Mt and (d) Gly-Mt with 10,000 $\times$  magnification.

The surface morphologies of the Mt and amino acid modified Mts were compared by SEM analyses. The SEM micrographs are shown at Fig 4 for Mt, Gly-Mt, Lys-Mt and Glu-Mt, respectively. It was clearly observed that the modified Mts surfaces exhibited a rough surface after this modification step. The clay platelets were stacked together in a disordered pattern to form agglomerates in some parts, and small and well-separated particles were also observed. These changes in the morphologies indicate that the intercalation was accompanied.

### 3.2 Electrochemical Characterization

In order to investigate the surface characterization and electron transfer mechanisms of different clay mineral surfaces, CV and Electrochemical Impedance Spectroscopy (EIS) techniques were utilized. As it is well known, EIS is an effective method for monitoring electrode surfaces after modification. Fig 5 demonstrates the Nyquist diagrams of bare GCE, amino acid modified and pristine Mt for 5.0 mM  $[\text{Fe}(\text{CN})_6]^{3-/4-}$ . As can be seen from the Fig 5, Gly-Mt clay mineral film modified GCE has the smallest semicircle diameter meaning has the fastest electron transfer compared to Lys-Mt and Glu-Mt. This situation was supported with cyclic voltammograms that were obtained with these electrodes for 5.0 mM  $[\text{Fe}(\text{CN})_6]^{3-/4-}$  at a scan rate of 50  $\text{mV s}^{-1}$  (Fig 6 a and Table 1). As can be seen from the Figure and the Table, Gly-Mt has the narrowest  $\Delta E$  values with a smaller formal potential a value demonstrating again the fastest electron transfer among all electrode types. Following these findings, the effect of scanning rate on CV voltammograms was examined by using Gly-Mt modified GCE (Fig 6 b). The CV measurements were carried out with varying scan rate between 5.0 – 1000  $\text{mV s}^{-1}$  and potential range of -0.4 – 0.8 V. As a result, it was observed that developed system has diffusion controlled behavior between 5.0 – 1000  $\text{mV s}^{-1}$  scan rates with an equation of  $y = 2.4708x + 10.588$ ,  $R^2 = 0.984$  for anodic and equation of  $y = -2.493x - 11.95$ ,  $R^2 = 0.965$  for cathodic. The range of scan rate is obviously wider than other Mt modified electrode surfaces as mentioned 5.0 – 200  $\text{mV s}^{-1}$  and 5.0 – 100  $\text{mV s}^{-1}$ ,<sup>12,3</sup>

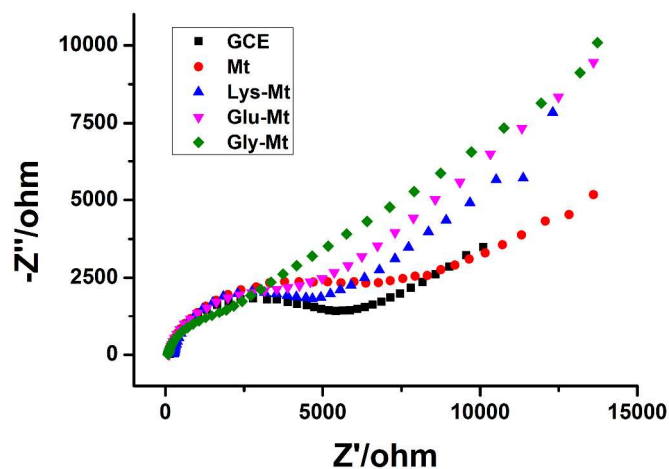


**Figure 5.** Nyquist plots of EIS for bare GCE and amino acid modified Mt electrodes in the presence of 5.0 mM  $[\text{Fe}(\text{CN})_6]^{3-/4-}$  and 0.1 M KCl in 50 mM sodium phosphate buffer (pH 6.5) at 0.2 V between 0.1 Hz- 100 kHz.

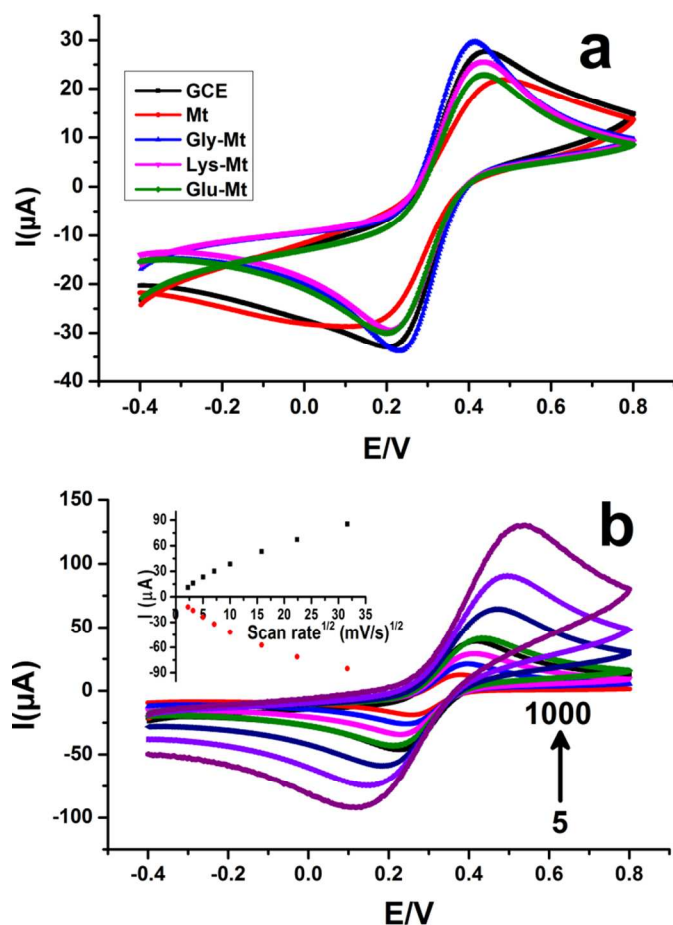


**Figure 6.** a) Cyclic voltammograms of pristine and modified Mts. [in 5.0 mM  $[\text{Fe}(\text{CN})_6]^{3-/4-}$  at a scan rate of  $50 \text{ mV s}^{-1}$ ]. b) Cyclic voltammograms of Gly-Mt at increasing scan rates [Inset graph shows the correlation between the current and square root of the scan rates (5; 10; 25; 50; 100; 250; 500;  $1000 \text{ mV s}^{-1}$ )].

**Table 1.** Summary of cyclic voltammetric data for modified electrodes.

	$E_{pa}(\text{V})$	$E_{pc}(\text{V})$	$\Delta E(\text{V})$	$E^{\circ}(\text{V})$
Gly-Mt	0.425	0.225	0.200	0.100
GCE	0.475	0.175	0.300	0.150
Lys-Mt	0.450	0.200	0.250	0.125
Glu-Mt	0.450	0.200	0.250	0.125
Mt	0.487	0.125	0.362	0.181

$$E^{\circ} = (E_{pa} + E_{pc}) / 2$$

### 3.3 Optimization and Analytical Characterization of A. A-Mt Biosensors

Initially, the pH of the medium was optimized *via* sodium acetate buffer (between pH 3.5 – 5.5) and citrate buffer (pH 2.5 – 3.0). Optimum pHs of different A. A-Mt/GOx biofilms were found as 3.5 for Lys-Mt and 4.0 for Gly-Mt and Glu-Mt, respectively (Fig 7). Afterwards, calibration curves for the each

biosensor were plotted at their optimum pHs. It is also known that the pH optimum of GOx as a free enzyme is 5.5 and in the previous work, when alkyl-amine intercalated Mts was used for the construction of GOx biosensor, optimum pH of the system was shifted to pH 4.0.<sup>12</sup>

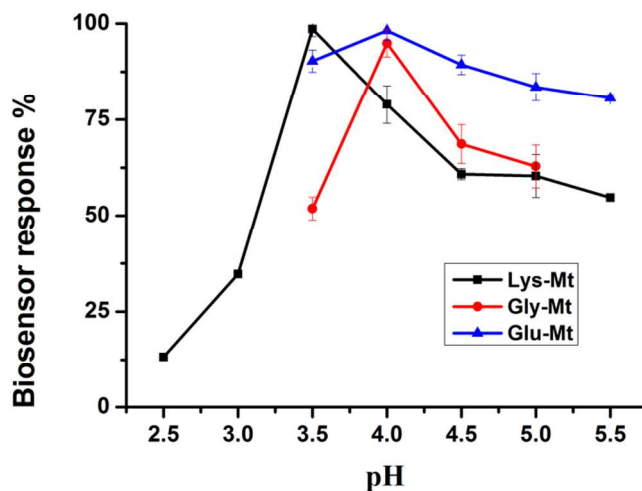


**Figure 7.** Effect of pH on the response of clay mineral-based GOx biosensors [in 50 mM sodium acetate buffer; at the ambient conditions. Electrode composition: GOx (0.5 mg), GA (2.5  $\mu\text{L}$ , 5.0% in pH 7.0, sodium phosphate buffer) and BSA (2.5  $\mu\text{L}$ , 1.0  $\text{mg mL}^{-1}$  in pH 7.0 sodium phosphate buffer) clay mineral (5.0  $\mu\text{L}$ , 1.0  $\text{mg mL}^{-1}$ , in pH 7.0, sodium phosphate buffer)].

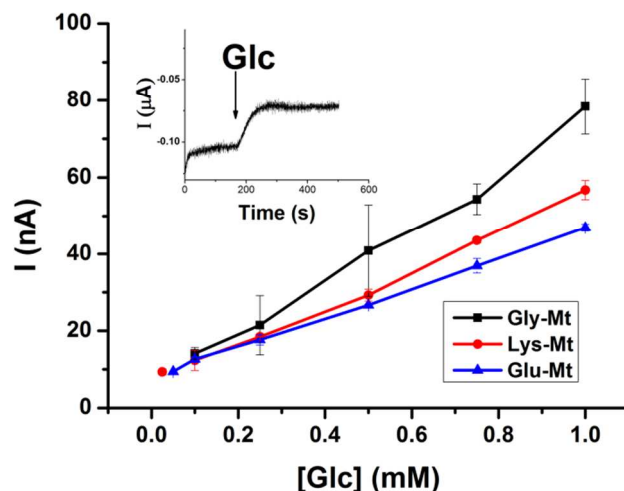


**Figure 8.** Effect of amino acid modifiers within calibration curves [at -0.7 V and ambient conditions, 50 mM, sodium-acetate buffer for Gly, Glu-Mt/GOx and sodium citrate buffer for Lys-Mt/GOx].

After determining the buffer conditions for each biosensing platform, calibration curves were formed *via* Gly, Lys and Glu-Mt. As shown in Fig 8 higher current values were obtained

from Gly-Mt/GOx sensor with a 30 s response time. The inset graph demonstrates the current response of the successive addition of 0.5 mM glucose. Some important analytical parameters for Gly-Mt/GOx are 0.1 – 1.0 mM as linear range,  $y = 70.573x + 5.148$  ( $R^2 = 0.990$ ) as a linear equation and  $K_m^{app} = 0.7$  mM (Michaelis-Menten constant)  $I_{max} = 107.8$  nA as kinetic parameters calculated from Lineweaver-Burk diagram for immobilized enzyme. Additionally, although Lys and Glu-Mt has wider detection range, their slopes ( $y = 48.716x + 6.974$ ,  $R^2 = 0.996$  for Lys-Mt/GOx and  $y = 38.78x + 9.112$ ,  $R^2 = 0.999$  for Glu-Mt/GOx) are lower than Gly-Mt/GOx electrode. Furthermore, a biofilm prepared with pristine Mt and plain biofilm generated from GA and BSA) had been carried out during the study. However, stability and repeatability of these biofilms were not good. The detection range of the constructed biosensors is lower than other clay-GOx biosensors fabricated with  $Ru(NH_3)_6^{3+}$  impregnated Mt structure (detection range: 1.0 – 15 mM)<sup>34</sup>. Furthermore, another GOx sensor based on ruthenium (II) complexes of thiosemicarbozones was reported and its linear range was 0.05 – 0.5 mM<sup>35</sup>. Additionally, amine-functionalized naphthalene containing conducting polymer based GOx biosensor<sup>36</sup> was constructed by Azak et al. and its linearity was between 0.05 and 1.0 mM which is similar to the Gly-Mt/GOx biofilm and dimethylamine intercalated Mt/GOx biosensor<sup>12</sup>.

Moreover, operational stability and repeatability were also investigated for Gly-Mt/GOx electrode. In the operational stability, 65 consecutive trials were performed by adding to reaction cell 0.5 mM glucose and a 53.8% decrease was observed in current responses after 9 h. For the repeatability, after 10 successive measurements using 0.5 mM glucose, the standard deviation (S.D) and variation coefficient (c.v) were calculated as  $0.45 \pm 0.01$  mM and 3.98%, respectively.

### 3.4 Sample Application

At the end of the study, sample application was accomplished for glucose analysis in some beverages such as coke, cherry juice and fizzy. Samples were directly applied to fabricate biosensor without any pre-treatment. The glucose contents were calculated using the signals from the linear equation for Gly-Mt/GOx and shown in Table 2. To compare the results, a spectrophotometric method was carried out with the same samples using a commercial glucose assay kit that includes Trinder reagent. Each data was given as the mean of 3 measurements  $\pm$ S.D. Recovery values indicate that the proposed biosensor can be used in glucose analysis of real samples.

**Table 2.** Glucose content of samples obtained by the Gly-Mt/GOx biosensor and reference method

Sample	Gly-Mt/GOx (M $\pm$ SD)	Trinder Reagent (M $\pm$ SD)	Recovery %
Coke	0.055 $\pm$ 0.002	0.059 $\pm$ 0.007	93.2
Cherry Juice	0.091 $\pm$ 0.007	0.098 $\pm$ 0.003	92.9
Fizzy	0.081 $\pm$ 0.005	0.086 $\pm$ 0.009	94.2

## 4 Conclusion

Inorganic matrices are alternatively used for organic polymers which are used widely for immobilizing biomolecules. Clay minerals like Mt provide fast, easy and inexpensive immobilization, high swelling and good capacity of cation alteration for biosensor applications.<sup>35</sup> Amino acid modified Mt has an important biodegradable property and low toxicity and other proper construction.<sup>29</sup> In this study, Glu-Mt, Lys-Mt and Gly-Mt were prepared and characterized. High intercalation yield was observed for the Gly-Mt modification. Moreover, the best biosensing performance was observed by using Gly-Mt biocomposite as the biosensor matrix in compared to the other A. A-Mt/GOx biosensors. Therefore, it can be concluded that Gly-Mt/GOx biosensor can be a good candidate for bioanalytical and biotechnological applications.

## Acknowledgements

Authors thank to Prof. C. Guler for the fruitful discussions during the characterization of clay matrices.

## Notes and references

<sup>a</sup> Ege University, Faculty of Sciences, Biochemistry Department, 35100-Bornova, Izmir, TURKIYE.

<sup>b</sup> Ege University, Faculty of Sciences, Chemistry Department, 35100-Bornova, Izmir, TURKIYE.

<sup>c</sup> Mugla Sitki Kocman University, Faculty of Sciences, Chemistry Department, Kotekli, Mugla, TURKIYE.

- H. Barhoumi, A. Maaref, M. Rammah, C. Martelet, N. Jaffrezic, C. Mousty, S. Vial and C. Forano, *Mater. Sci. Eng. C*, 2006, **26**, 328.
- A. Mignani, E. Scavetta and D. Tonelli, *Anal. Chim. Acta*, 2006, **577**, 98.
- B. Demir, M. Selecı, D. Ag, S. Cevik, E. E. Yalcinkaya, D. Odacı Demirkol, U. Anik and S. Timur, *RSC Adv.*, 2013, **3**, 7513.
- R. Bongartz, D. Ag, M. Selecı, J.G. Walter, E. E. Yalcinkaya, D. Odacı Demirkol, F. Stahl, S. Timur and T. Scheper, *J. Mater. Chem. B*, 2013, **1**, 522.
- D. Depan, A. P. Kumar and R. P. Singh, *Acta Biomater.*, 2009, **5**, 93.
- K-H. Liu, T-Y. Liu, S-Y. Chen and D-M. Liu, *Acta Biomater.*, 2008, **4**, 1038.
- S. Gopinath and S. Sugunan, *Appl. Clay Sci.*, 2007, **35**, 67.

- 8 C. Mousty, *Appl. Clay Sci.*, 2004, **27**, 159.
- 9 E. Zappa, D. Brondania, I. C. Vieira, C. W. Scheeren, J. Dupont, A. M. J. Barbosa and V. S. Ferreira, *Sens. Actuators B*, 2011, **155**, 331.
- 10 J-Y. Chiou, R-S. Hsu, C-W. Chiub and J-J. Lin, *RSC Adv.*, 2013, **3**, 12847.
- 11 K. Khezri, V. Haddadi-Asl, H. Roghani-Mamaqani and M. Salami-Kalajahi, *J. Polym. Res.*, 2012, **19**, 9868.
- 12 M. Seleci, D. Ag, E. E. Yalcinkaya, D. Odaci Demirkol, C. Guler and S. Timur, *RSC Adv.*, 2012, **2**, 2112.
- 13 M. Alexandre and P. Dubois, *Mater. Sci. Eng. R*, 2000, **28**, 1.
- 14 A. Fudala, I. Palinko and I. Kiricsi, *Inorg. Chem.*, 1999, **38**, 4653.
- 15 C. Lei and J. Deng, *Anal. Chem.*, 1996, **68**, 3344.
- 16 S. Poyard, N. Jaffrezic-Renault, C. Martelet, S. Cosnier, P. Labbe and J. L. Besombes, *Sens. Actuators B*, 1996, **33**, 44.
- 17 M. E. Ramos and F. J. Huertas, *Appl. Clay Sci.*, 2013, **80–81**, 10.
- 18 S. Sato, *Clays Clay Miner.*, 1999, **47**, 793.
- 19 S. Aisawa, S. Sasaki, S. Takahashi, H. Hirahara, H. Nakayama and E. Narita, *J. Phys. Chem. Solids*, 2006, **67**, 920.
- 20 S. P. Newman, T. D. Cristina, V. Coveney and W. Jones, *Langmuir*, 2002, **18**, 2933.
- 21 Q. Yuan, M. Wei, D. G. Evans and X. Duan, *J. Phys. Chem. B*, 2004, **108**, 12381.
- 22 S. Mallakpour and S. Moslemi, *Prog. Org. Coat.*, 2012, **74**, 8.
- 23 A. Avinash, D. R. Katti and K. S. Katti, *Mater. Sci. Eng. C*, 2011, **31**, 1017.
- 24 M. Wang, Q. Hu, D. Liang, Y. Li, S. Li, X. Zhang, M. Xi and X. Yang, *Appl. Clay Sci.*, 2013, **83–84**, 182.
- 25 D. Songurtekin, E. E. Yalcinkaya, D. Ag, M. Seleci, D. Odaci Demirkol and S. Timur, *Appl. Clay Sci.*, 2013, **86**, 64–69.
- 26 E. E. Saka and C. Guler, *Clay Miner.*, 2006, **41**, 853.
- 27 L. C. Clark Jr. and C. Lyons, *Ann. N. Y. Acad. Sci.*, 1962, **102**, 29.
- 28 P. Trinder, *Ann. Clin. Biochem.*, 1969, **6**, 24.
- 29 S. Mallakpour and M. Dinari, *Appl. Clay Sci.*, 2011, **51**, 353.
- 30 E. E. Yalcinkaya and C. Guler, *Sep. Sci. Technol.*, 2010, **45**, 635.
- 31 M. Bauman, A. Kosak, A. Lobnika, I. Petrinic and T. Luxbacher, *Colloids Surf. A*, 2013, **422**, 110.
- 32 J. Yang and D. Y. Kwok, *Anal. Chim. Acta*, 2004, **507**, 39.
- 33 C. Werner, U. Konig, A. Augsburg, C. Arnhold, H. Korber, R. Zimmermann and H-J. Jacobasch, *Colloids Surf. A*, 1999, **159**, 519.
- 34 T. Ohsaka, Y. Yamaguchi and N. Oyama, *Bull. Chem. Soc. Jpn.*, 1990, **63**, 2646.
- 35 H. Yildirim, E. Guler, M. Yavuz, N. Ozturk, P. Kose Yaman, E. Subasi, E. Sahin and S. Timur, *Mater. Sci. Eng. C*, 2014, **44**, 1.
- 36 H. Azak, E. Guler, U. Can, D. Odaci Demirkol, H. B. Yildiz, O. Talaz and S. Timur, *RSC Advances*, 2013, **3**, 19582.
- 37 C. Mousty, *Anal. Bioanal. Chem.*, 2010, **396**, 315.